BULLETIN OF THE EARTHQUAKE
RESEARCH INSTITUTE
Vol. 44 (1966), pp. 873-891

45. *Frequency Analysis of Seismic Waves (1)*

By Masaru TSUJIURA,

Earthquake Research Institute.

(Read Feb. 22, 1966.-Received June 30, 1966.)

Abstract

The frequency spectra of body waves from near and distant earthquakes are investigated by the use of a set of analogue band-pass filters, each having an octave band width in frequency. The seismic waves are separated into five frequency bands ranging from 0.5 to 40 cycles per second. The filtered wave signals are amplified and recorded continuously on a multi-channel ink-writing oscillograph.

Some of the results of the present analysis based on the observations since December, 1965 may be summarized as follows.

1) From the attenuation curves of the amplitude ratio of two different frequency bands obtained from many near earthquakes, the minimum Q value of P waves in the earth's crust and the upper-most mantle is estimated at about 500.

2) The ratio of the spectral amplitude of the teleseismic P waves at 2 cps to that at a lower frequency than 1 cps increases generally with the focal depth. A remarkable fact is that the amplitude ratio for earthquakes with the focal depth from 100 to 200 km in Fiji Islands is small as compared with that for the other focal depth ranges suggesting a possible effect of the low velocity channel. On the contrary, two exceptional shocks in Central Asia with shallow depths indicate a larger amplitude ratio at 2 cps channel than that of deep earthquakes and may be suggested as man-made explosions.

1. Introduction

We shall first describe our method for obtaining the spectrum of the body waves of near and distant earthquakes, and then investigate the relation between the spectra of the seismic waves and the magnitude of source, epicentral distance and focal depth.

In the course of this study, we shall obtain the value of the attenuation coefficient Q of the earth's crust. In order to estimate accurately the

value of Q, it is necessary to study the seismic waves from earthquakes with the same magnitude and different epicentral distances. It is necessary, for this purpose, to use various different seismographs with different magnification. However, we used one seismograph with a limited dynamic range in the present study, and we had to introduce some assumptions to get the Q value.

It will be shown that the fraction of high frequency components of the distant earthquakes, in general, decreases with the epicentral distance for a given focal depth, and it definitely increases with the focal depth for a given distance.

In order to investigate the problems mentioned above, the seismographs have been set up at Mt. Tsukuba located at about 60 km north-east of Tokyo since December, 1965. The output signals from the seismographs are sent to the receiving station at the Earthquake Research Institute building in Tokyo by a radio telemetering system. The use of the radio-telerecorder is not essential for the purpose of the present study but is very convenient and useful for having records always at hand in the practical processing. Moreover, Mt. Tsukuba is located near the center of the north-eastern part of the Kwanto district where seismicity is very high and, on the contrary, the noise level is very low, *ca.* 1 micro-kine at 6 cps in average, as the firm granitic basement is exposed on the surface in the area. So, the magnification of the seismograph can be set at a very high level. This makes our study efficient and also makes it possible to detect the frequency spectrum even for very small earthquakes.

2. Seismograph and Frequency Analyzer

2-1. Description of the seismograph and frequency analyzer

Fig. 1 shows the block diagram of the radio-telerecording seismograph system (RTS-II) representing schematically our instrumentation used for the present frequency analysis. In this paper we shall describe only the system of frequency analysis, as the other part of the instrumentation was reported before.[1) 2) 3)] The seismograph is set in a new vault in the campus of the Tsukuba Seismological Observatory of the Earthquake

1) S. MIYAMURA and M. TSUJIURA, *Bull. Earthq. Res. Inst.*, **35** (1957), 381-394.
2) M. TSUJIURA and S. MIYAMURA, *Bull. Earthq. Res. Inst.*, **37** (1959), 193-206.
3) K. AKI, H. MATUMOTO, M. TSUJIURA and T. MARUYAMA, *Bull. Earthq. Res. Inst.*, **43** (1965), 381-397.

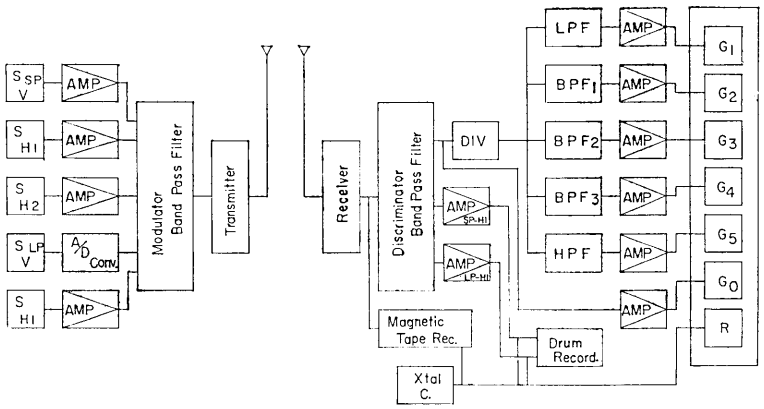

Fig. 1. Block diagram of the seismograph system and frequency analyzer.

S	: Seismometer	DIV	: Divider
V	: Vertical	LPF	: Low-pass filter
H	: Horizontal	BPF	: Band-pass filter
SP	: Short period	HPF	: High-pass filter
LP	: Long period	G	: Galvanometer
AMP	: Amplifier	R	: Relay

A/D Conv. : Analogue to Digital converter

Research Institute. The seismometer is a short-period vertical component type with free period of one second and its moving coil output is supplied to the amplifier. The output of the amplifier is frequency-modulated and sent by the radio-telemetering system to the receiving station set up at our institute building in Tokyo.

At the receiving station, the signal is discriminated by a frequency demodulator. The output of the demodulator is supplied to the divider which makes five identical outputs. These five outputs are supplied to the filters independently and they are amplified and recorded continuously by a multi-channel ink-writing oscillograph. Reading on the multi-channel record can be made more easily than on the separate drum records. Then, an average spectral amplitude with each frequency band is obtained directly from the record of the oscillograph. The paper speed of the recording oscillograph is 60 mm per minute. The galvanometer designated as Go in Fig. 1 with the power amplifier AMP records the original seismic signal with overall frequency characteristics as shown in Fig. 4.

In order to get the *S-P* time, the signal from a horizontal component seismograph is also telemetered from Tsukuba and recorded on a helical drum at the receiving station at a paper speed of 120 mm per minute.

The practical design of the frequency analyzer will be described in the following.

2-2. Construction of the frequency analyzer

The present writer is especially interested in the frequency spectra of small earthquakes with the frequency range from 1 cps to 50 cps, and also in the same frequency components of body waves from distant earthquakes.

For the spectral study of such waves, the automatic processing filters to separate the waves into five channels are designed and constructed. Fig. 2 shows the frequency characteristics of the filters.

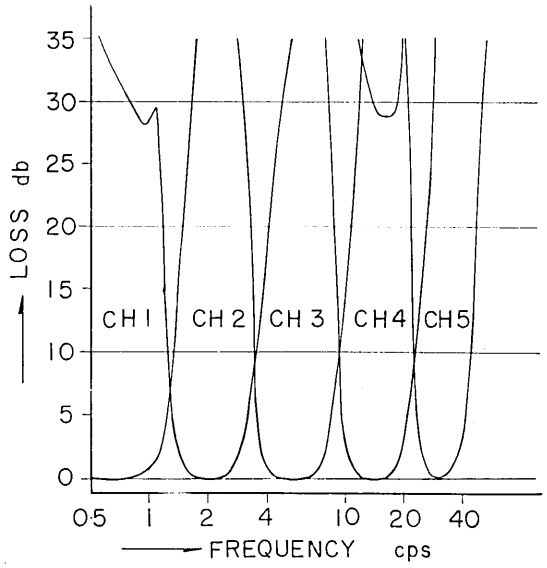

Fig. 2. Frequency characteristic curves of five filters.

Channel 1 is the low-pass filter with the cut-off frequency of 1 cps. From channel 2 to channel 4 are the band-pass filters which have the pass bands with one octave band width. Channel 5 is a simple high-pass filter with cut-off at 25 cps. Since the free period of the recording galvanometers of this system is 0.03 sec., the band width of the 5th channel is narrower than the other four channels. The band-pass filters consist of a low-pass and a high-pass filter which are C-R active filters with a feed back amplifier.

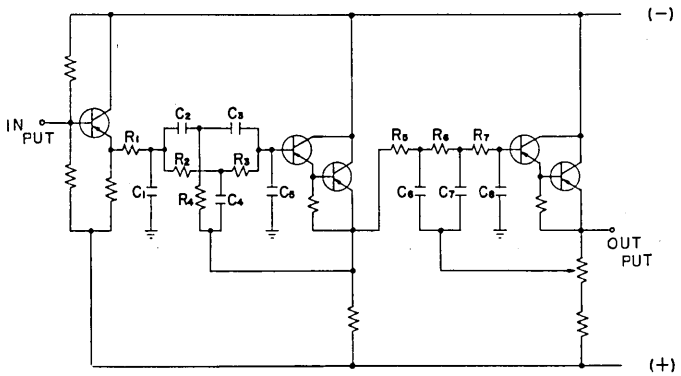

Fig. 3. Basic circuit of low-pass filter.

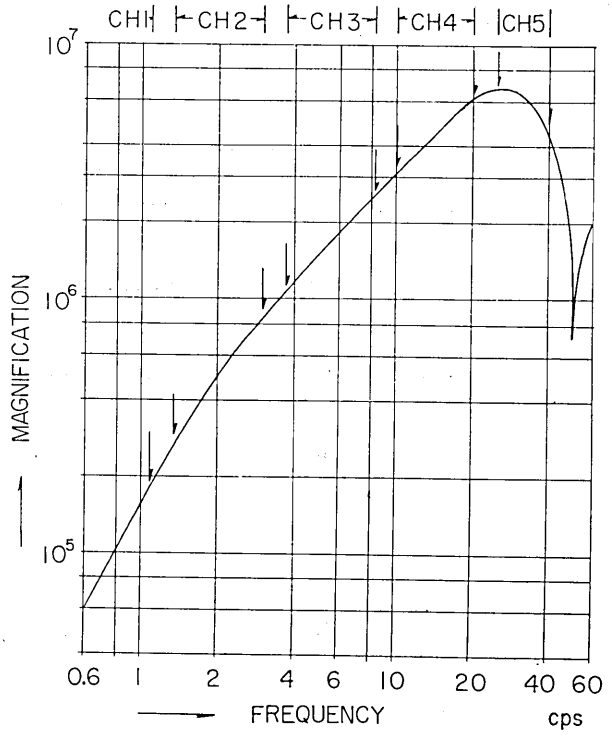

Fig. 4. Magnification curve of the seismograph.

The general idea of this circuit is due to McVey (1962).[4] But, we replaced vacuum tubes by transistors, and improved the side-lobe characteristics. As shown in Fig. 2, channel 1 is a single low-pass filter. Channel No. 2–4 are the band-pass filters, a combination of high-pass and low-pass filters. The circuit of the high-pass filter will be identical to that of the low-pass filter, if we interchange the resistance and the condenser in Fig. 3.

Fig. 4 shows the over-all magnification of the system. The frequency ranges indicated by the arrows in Fig. 4 represent the band widths and the channel numbers of the filters.

3. Frequency Analysis of Near Earthquake Waves

Fig. 5 shows examples of the filter outputs, recorded by a six-channel ink-writing oscillograph for some near earthquakes. In this figure, the numbers from 1 to 5 show the channel numbers. With the increase of the channel numbers, the frequency of the waves becomes higher as men-

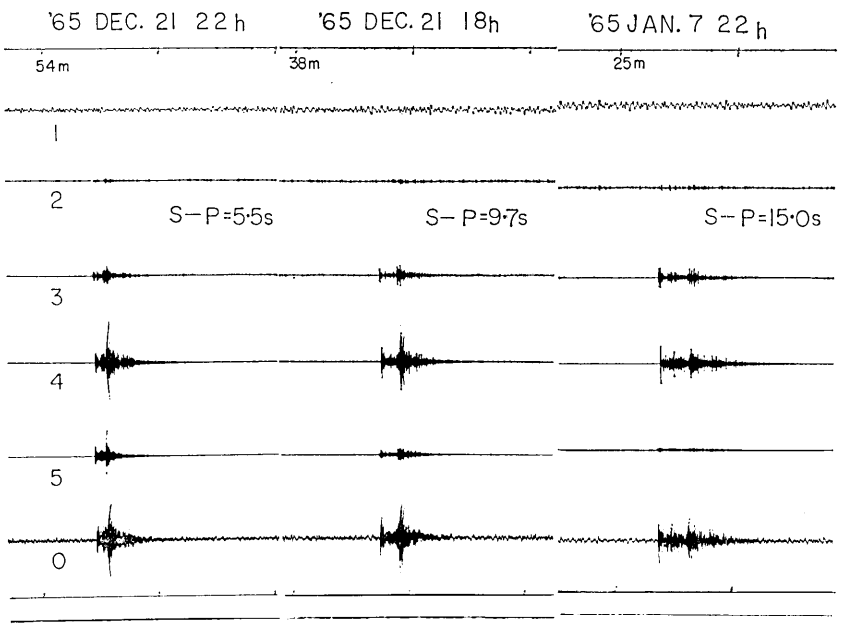

Fig. 5. An example of the frequency-analyzed data of near earthquakes.

4) P. J. W. McVEY, *Electronic Engineering*, **34** (1962), 458–463.

tioned before. The record of the number 0 indicates the original record which corresponds to the sum of outputs of the channels from 1 to 5. As is shown in Fig. 5, the amplitudes for these near earthquakes are always greatest in channel 4, which has the central frequency of 15 cps. The higher frequency components in channel 5 decrease with the increase of the *S-P* time. In other words, the amplitude ratio of channel 5 to channel 4 (CH5/CH4) becomes smaller with the increase of the *S-P* time. The amplitude ratio of channel 4 to channel 3 (CH4/CH3) decreases also with the increase of the *S-P* time.

Initial motions of *P* waves from such near earthquakes in channel 2 and 1 are small as compared with those of the other channels, the noise being larger than that found in other channels. Therefore the ratio of the signal to noise is very small. The major parts of the noises of these two channels are the microseisms, these noises being found even on a quiet day. Therefore we cannot read the amplitudes of channels 1 and 2 for small earthquakes.

We classified about 600 observed earthquakes with respect to their *S-P* times ranging from 5.0 to 21.9 sec into 17 groups with 1 sec step.

Next, we measured the maximum amplitudes of *P* and *S* wave groups of each channel.

Then, we averaged the trace amplitudes of that channel within each of the earthquake group classified above.

Table 1 shows the averaged amplitude in mm on the record as well as the corresponding ground velocity in μ kine (micro-kine), or 10^{-6} cm/sec.

Finally, we took the ratio of the average amplitude for each channel to that of channel 4.

As a typical example, an average frequency spectrum of 39 earthquakes with *S-P* times between 9.0 and 9.9 sec is shown in Fig. 6. The curves drawn in solid lines are obtained from the initial *P* wave, and those in dotted lines from *S* wave. It clearly indicates that the amplitudes of the low frequency components are smaller than those of the high frequency components for smaller earthquake.

As shown in Table 1 in Gothic character, the maximum amplitude is found without exception in channel 4 when the *S-P* time is between 5.0 to 17.0 sec. However, for the earthquakes which have longer *S-P* times, the channel of the maximum amplitude is shifted to lower frequency channels.

The frequency spectra of *S* waves of near earthquakes are also obtained in the same way as those of *P* waves. But it is difficult to iden-

Table 1. a

CH	1		2		3		4		5		n	M
BW	1		1.7		4.5		10		16			
S-P CF in sec	0.75		2.1		6		15		32			
	A	V	A	V	A	V	A	V	A	V		
5.0— 5.9	—	—	—	—	7.7	15.3	**17.6**	**35.2**	9.7	29.2	17	1.0
6.0— 6.9	—	—	—	—	6.5	13.1	**15.2**	**30.4**	9.4	28.3	17	1.1
7.0— 7.9	—	—	—	—	10.0	20.0	**17.5**	**35.0**	8.4	25.4	35	1.3
8.0— 8.9	—	—	0.8	2.1	7.8	15.5	**13.3**	**26.6**	5.5	16.6	39	1.4
9.0— 9.9	—	—	1.2	2.9	5.3	10.6	**10.0**	**20.0**	3.7	11.2	39	1.5
10.0—10.9	—	—	1.8	4.5	7.6	15.3	**11.1**	**22.2**	3·2	9.5	33	1.6
11.0—11.9	—	—	1.6	3.9	8.2	16.4	**11.7**	**23.4**	3.3	9.9	20	1.7
12.0—12.9	—	—	2.2	5.5	8.9	17.9	**10.7**	**21.4**	3.3	9.9	23	1.8
13.0—13.9	—	—	1.5	3.7	5.8	11.6	**6.9**	**13.8**	1.8	5.3	27	1.9
14.0—14.9	—	—	1.5	3.6	10.8	21.6	**15.0**	**30.0**	4.0	12.0	11	2.0
15.0—15.9	—	—	2.2	5.5	7.6	15.2	**10.1**	**20.2**	2.0	6.0	16	2.1
16.0—16.9	—	—	1.6	4.1	8.8	17.6	**13.7**	**27.4**	3.8	11.3	8	2.1
17.0—17.9	—	—	1.9	4.6	7.8	15.6	**8.6**	**17.2**	1.6	4.8	18	2.2
18.0—18.9	—	—	1.7	4.1	**7.8**	**15.5**	6.4	12.9	0.9	2.6	20	2.2
19.0—19.9	—	—	1.6	3.9	**7.9**	**15.7**	6.7	13.3	1.0	3.1	49	2.3
20.0—20.9	—	—	2.3	5.8	**10.0**	**20.0**	7.7	15.5	0.9	2.7	115	2.3
21.0—21.9	—	—	3.6	9.1	**11.4**	**22.4**	9.5	18.9	1.1	3.3	24	2.4

Table 1. a. The averaged amplitude spectrum of the *P* waves in mm on the record as well as the corresponding ground velocity in μkine (microkine), or 10^{-6} cm/sec.

CH : Channel number BW : Band width in cps
CF : Center frequency in cps
A : Trace amplitude in mm V : Ground velocity in μkine
n : Number of shocks M : Mean magnitude[5]

5) The mean magnitude was calculated based on the following equation

$$M=\log A+\alpha \log \triangle -r.$$

As for A in this equation, we used the mean amplitude of the ground motion of *S* phases (in micron) in channel 4 for all earthquakes in respective *S-P* intervals. We took the value of α as 2.2, which is adopted by J.M.A. for Mt. Tsukuba, and the epicentral distance (in km) as $\triangle=k\times(S-P)$, where k=8.2 km per sec. The value of r was taken as zero in order to make the calculated magnitudes of several small earthquakes near Matsushiro consistent with those determined by the E.R.I. expedition team.

Table 1. b

CH	1		2		3		4		5		n	M
BW	1		1.7		4.5		10		16			
S-P CH	0.75		6		6		15		32			
in sec	A	V	A	V	A	V	A	V	A	V		
5.0— 5.9	—	—	2.2	5.5	10.1	20.2	**26.9**	**53.6**	13.8	41.4	12	1.0
6.0— 6.9	—	—	1.7	4.3	10.0	20.0	**22.6**	**45.2**	8.5	25.5	14	1.1
7.0— 7.9	—	—	3.1	7.7	12.1	24.2	**22.6**	**45.2**	6.2	18.6	30	1.3
8.0— 8.9	—	—	3.1	7.8	11.2	22.4	**22.8**	**45.6**	6.9	20.8	32	1.4
9.0— 9.9	—	—	2.4	5.9	11.7	23.4	**17.6**	**35.2**	5.2	15.6	33	1.5
10.0—10.9	—	—	4.6	11.8	14.5	29.0	**17.7**	**35.4**	5.4	16.4	31	1.6
11.0—11.9	—	—	3.6	9.0	10.6	21.2	**16.3**	**32.6**	3.4	10.2	15	1.7
12.0—12.9	—	—	6.5	16.3	11.9	23.8	**17.7**	**35.4**	3.5	10.5	16	1.8
13.0—13.9	—	—	8.9	22.1	15.0	30.0	**19.2**	**38.4**	3.1	9.3	21	1.9
14.0—14.9	—	—	4.0	9.9	12.8	25.5	**16.4**	**32.8**	3.3	10.0	11	2.0
15.0—15.9	—	—	7.7	19.1	21.2	42.4	**21.3**	**42.6**	3.8	11.4	17	2.1
16.0—16.9	—	—	1.8	4.4	9.2	18.4	**13.8**	**27.6**	2.6	7.9	4	2.1
17.0—17.9	—	—	3.5	8.8	**12.0**	**24.0**	10.4	20.8	1.7	5.0	12	2.2
18.0—18.9	—	—	3.9	9.8	**13.7**	**27.4**	8.9	17.8	1.2	3.5	19	2.2
19.0—19.9	—	—	5.0	12.5	**18.1**	**36.2**	14.2	28.4	1.5	4.4	46	2.3
20.0—20.9	—	—	4.9	12.3	**16.4**	**32.8**	12.3	24.6	1.1	3.3	98	2.3
21.0—21.9	—	—	5.6	14.1	**17.6**	**35.2**	12.7	25.4	1.2	3.5	24	2.4

Table 1. b. The averaged amplitude of the *S* waves in mm on the record as well as the corresponding ground velocity in μkine (micro-kine), or 10^{-6} cm/sec.

CH : Channel number
CF : Center frequency in cps
A : Trace amplitude in mm
n : Number of shocks
BW : Band width in cps
V : Ground velocity in μkine
M : Mean magnitude

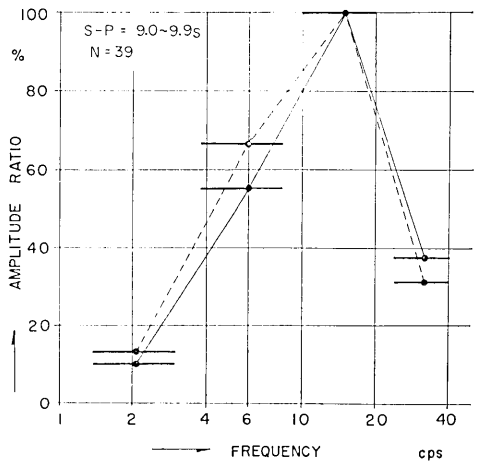

Fig. 6. Average amplitude spectrum of 39 earthquakes with *S-P* time between 9.0 and 9.9 sec.

tify the *S* phase exactly for larger *S-P* times because we used a vertical seismograph. Therefore, these values may be less reliable than those of *P* phase.

In order to estimate the attenuation coefficient *Q*, we shall investigate the amplitude ratio for the two different frequencies as a function of the epicentral distance. The method of measuring the amplitude ratios is as follows:—

Firstly, we classify earthquakes according to the *S-P* time ranging from 5.0 to 21.9 sec into 17 groups each with 1 sec interval in the same way as mentioned before.

Secondly, we take the amplitude ratio between the two channels for each earthquake. Thirdly, we calculate the mean amplitude ratio for each of the earthquake group. For example, the amplitude ratio of channel 4 to channel 3 is indicated as CH4/CH3. If we denote this ratio as A_i/B_i for the *P* wave of the *i*-th earthquake, the mean value *b* is defined as

$$b=\frac{a}{n},$$

where

$$a=\frac{A_1}{B_1}+\frac{A_2}{B_2}+\cdots+\frac{A_n}{B_n}.$$

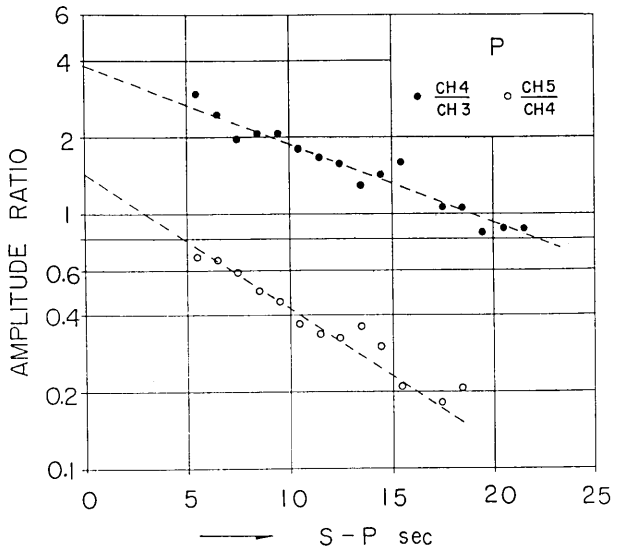

Fig. 7. The average amplitude ratio between two different frequency bands for the near earthquakes.

Fig. 7 shows the values of b obtained from the trace amplitude of P waves of the earthquakes with the S-P time ranging from 5.0 to 21.9 sec. The closed circle shows the amplitude ratio of CH4/CH3, and the open circle shows that of CH5/CH4 respectively. Since we are using a seismograph with a limited dynamic range, the magnitude of earthquakes selected in our analysis tends to increase with the increase of S-P time. However, if we assume that the mean amplitude ratio between different frequencies does not depend on the magnitude of earthquake, we may take Fig. 7 as showing the effect of attenuation on P waves. Then we can calculate the Q values of the attenuation from the figure.

The equation for the attenuation of the waves may be written in the form

$$A=A_0 e^{-\frac{\pi t}{QT}}, \tag{1}$$

where t and T are travel time and period respectively and A_0 and Q are constants. If we put the average velocity of P waves V, then

$$A=A_0 e^{-\frac{\pi x}{QVT}} \tag{2}$$

If we estimate the distance x from the S-P time by the formula $x=V_{s-p}\cdot t_{s-p}$, the amplitude of P waves at a certain epicentral distance may be written as

$$A_{(T)}=A_{0(T)}e^{-\frac{\pi V_{s-p}}{QV}\cdot\frac{t_{s-p}}{T}} \tag{3}$$

Then, the amplitude ratio of two different periods T_1 and T_2 of P waves at a certain epicentral distance will take the following form

$$\frac{A_{(T_1)}}{A_{(T_2)}}=\frac{A_{0(T_1)}}{A_{0(T_2)}}e^{-\frac{\pi V_{s-p}}{QV}\cdot\left(\frac{1}{T_1}-\frac{1}{T_2}\right)\cdot t_{s-p}} \tag{4}$$

Taking the logarithm of eq. (4),

$$\log_{10}\frac{A_{(T_1)}}{A_{(T_2)}}=\log_{10}\left(\frac{A_{0(T_1)}}{A_{0(T_2)}}\right)-\log_{10}e\cdot\frac{\pi V_{s-p}}{QV}\cdot\left(\frac{1}{T_1}-\frac{1}{T_2}\right)\cdot t_{s-p} \tag{5}$$

The second term of right-hand side of this equation indicates the attenuation of seismic waves, and the slope of attenuation curves in Fig. 7 is equal to

$$\log_{10}e\cdot\frac{\pi V_{s-p}}{QV}\cdot\left(\frac{1}{T_1}-\frac{1}{T_2}\right).$$

Thus the value of Q can be obtained from this equation. If we draw dashed lines as indicated in Fig. 7 for average slopes, the values of Q are obtained as 560 and 535 from the upper and lower curves respectively.

We assumed that the mean amplitude ratio between different frequencies does not depend on the magnitude of earthquakes. However, we are taking larger earthquakes with the increase of S-P time. The relation between the spectra and the magnitude of earthquakes is not yet obtained in detail as the dynamic range of our seismograph is limited. However, from the result of analyzed data it may be suggested that the low frequency components increase with increase of the magnitude of source as pointed out by T. Matumoto (1960).[6] Therefore, if we correct for this magnitude effect, the slope of the curves in Fig. 7 should become more gentle than shown there, and the value of Q will become larger than those given before. In other words, our values may be the minimum estimate.

6) T. MATUMOTO, *Bull. Earthq. Res. Inst.*, 38 (1960), 13-27.

4. Frequency Analysis of Distant Earthquake Waves

We also investigate the spectra of P waves from distant earthquakes by the same method as applied to those from the near earthquakes. It is well known that the predominant period of P waves increases with the increase of the magnitude of source. The predominant period of P waves for the earthquakes with magnitude around 5 is about 1 sec as reported by K. Kasahara (1957)[7] and B. Gutenberg (1958).[8] Therefore, our analyser will cover the predominant frequency if we use the data from these small earthquakes. After travelling over a long distance in the mantle, the amplitude spectrum of P waves of such earthquakes would provide us with

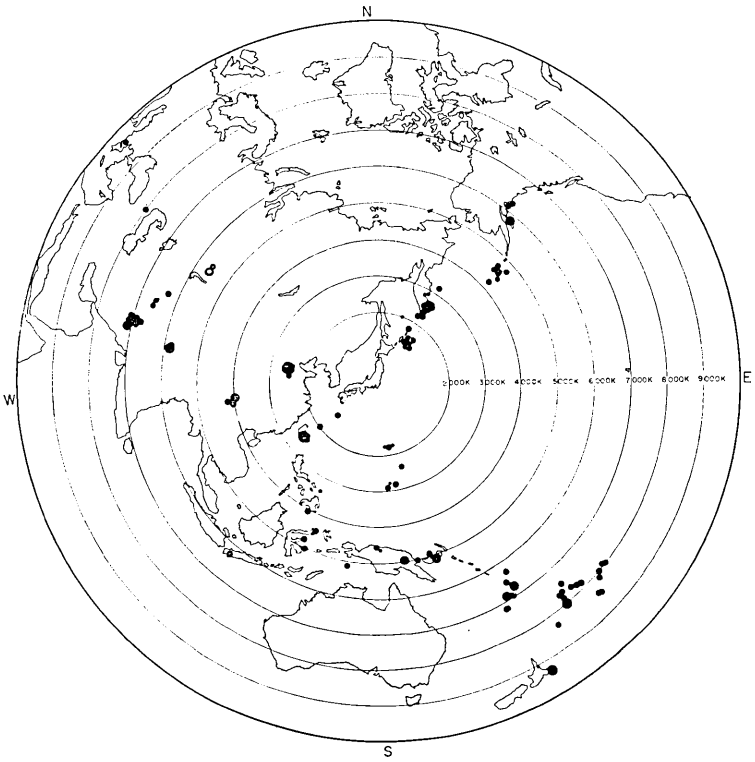

Fig. 8. Epicentral location of earthquakes which were analyzed by our method in the period from December 1965 to March 1966.

7) K. KASAHARA, *Bull. Earthq. Res. Inst.*, **35** (1957), 473-532.
8) B. GUTENBERG, *Bull. Seism. Soc. Amer.*, **48** (1958), 269-282.

valuable information for the determination of the value of Q in the mantle.

As pointed out by T. Asada and K. Takano (1963),[9] the P waves from deep shocks contain, on the average, higher frequency waves than shallow shocks. From this point of view, we take notice at first of the difference of the spectra of P waves between the earthquakes with different focal depth in various regions.

Fig. 8 shows epicentres of earthquakes selected for our analysis. The number of shocks is not yet enough to calculate the Q value, since only in Dec. 1965 was the continuous observation started. So, we investigate, for the present, the difference between spectral curves of P waves of earthquakes which occurred in various focal depths in some selected regions.

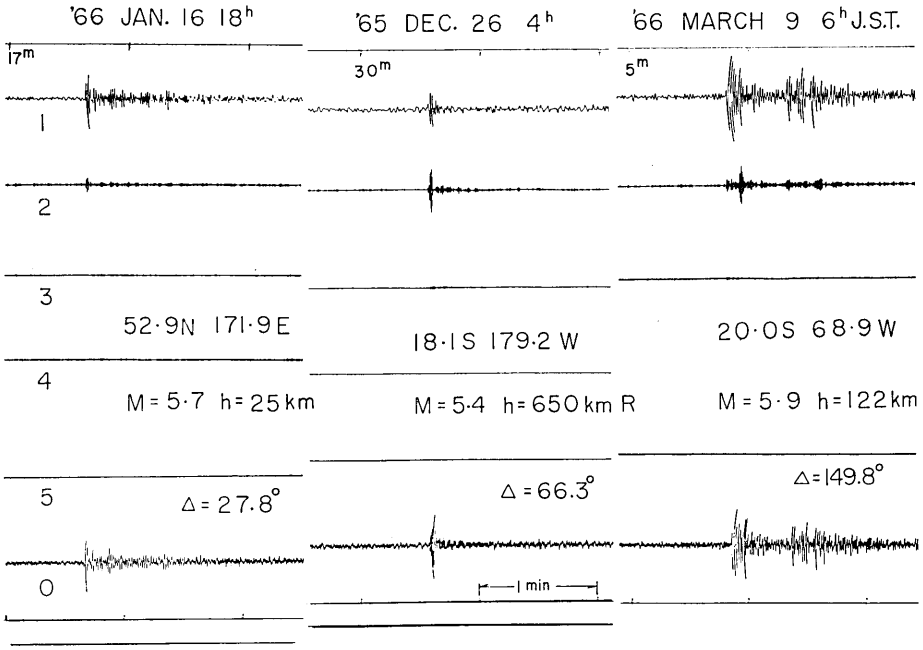

Fig. 9. Typical example of the result of frequency analysis of the distant earthquakes.

A result of the analysis is shown in Fig. 9. The number from 1 to 5 indicates the channel number. The frequency band widths are the same as for the analysis of the near earthquakes which are given in the previous

9) T. ASADA and K. TAKANO, *J. Phys. Earth*, **11** (1963), 25-34.

chapter. The original seismogram before filtering is indicated as channel 0. The location, magnitude (M) and focal depth (h) were found from the P.D.E. cards of the U.S.C.G.S.. There is a remarkable difference in the amplitude ratio of CH2/CH1 among different earthquakes as shown in Fig. 9.

Fig. 10 shows the amplitude ratio of channel 2 to channel 1, (CH2/CH1), for the earthquakes which took place in the Aleutian Islands region. The epicentral distances of these earthquakes are around 4200 km and the magnitudes from 5.2 to 5.7. As can be seen in Fig. 10, the amplitude

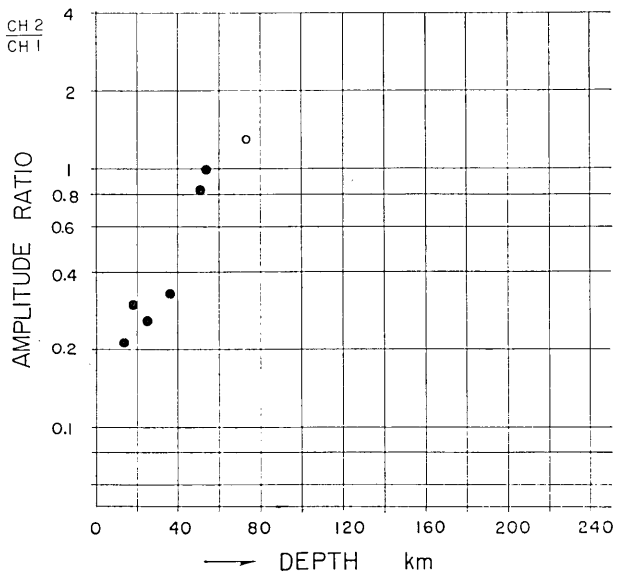

Fig. 10. The amplitude ratio between two different frequency bands for the *P* waves of distant earthquakes which took place in the Aleutian Islands region. Open circle indicates the earthquake of which the focal depth was not computed but assumed by the USCGS and shown as (R) in the PDE card.

ratio between the two channels increases with the increase of the focal depth. This means that the amplitude of the high frequency components of seismic waves increases with the increase of focal depth, and the focal depth where the amplitudes of the two channels come to be equal is about 50 km. It will be interesting to study the variation of the amplitude ratio for the shocks with deeper foci. However, such deep shocks have not yet been observed from this region.

Fig. 11 shows the amplitude ratio for the earthquakes which took place in the Fiji and Tonga Islands regions. The epicentral distances for these earthquakes are around 7500 km and the magnitude ranges from 5.3 to 5.8. As can be seen in this figure, the amplitude ratio also increases with the increase of focal depth. However, the slope of the curve is more gentle than the amplitude ratio for the Aleutian region. It is a remarkable fact that the amplitude ratio does not increase continuously with the focal depth, but that the amplitude ratio for the focal depth between about 100 and 200 km is very small in comparison with those for the other focal depth ranges.

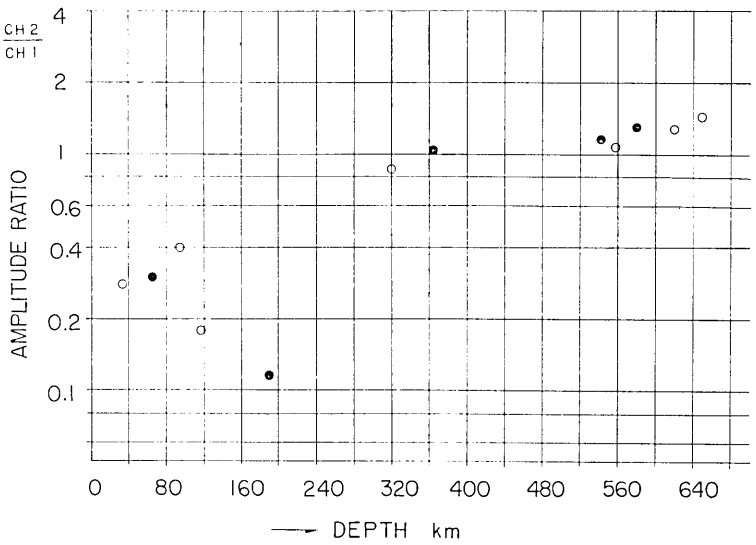

Fig. 11. The amplitude ratio between two different frequency bands for the *P* waves of distant earthquakes which took place in the Fiji and Tonga Island regions. Open circles indicate the earthquakes for which the focal depth was not computed but assumed by the USCGS and shown as (R) in the card.

A similar result was obtained from the spectrum of PKIKP phase for the same region by Mohammadioun (1965)[10] in the lower frequency ranges.

From these results, we may suggest that the relation between the spectrum and the focal depth may reflect the upper-mantle structure in the region. In fact, the model 8099 of the upper-mantle structure for the

10) B. MOHAMMADIOUN. *C. R. Acad. Paris*, **261** (1965), 4472-4474.

Pacific Ocean given by Dorman, Ewing and Oliver (1960)[11] includes the Gutenberg's low-velocity layer at the depth from 60 to 220 km. Therefore, this may indicate that the high frequency components are very small for the earthquakes which took place in the low-velocity layer. However, as shown in the figure, only two points are found with the small ratio. Therefore, we have to continue the observation and study more of the spectra of earthquakes in the region, as well as in the other regions where deep earthquakes are occurring.

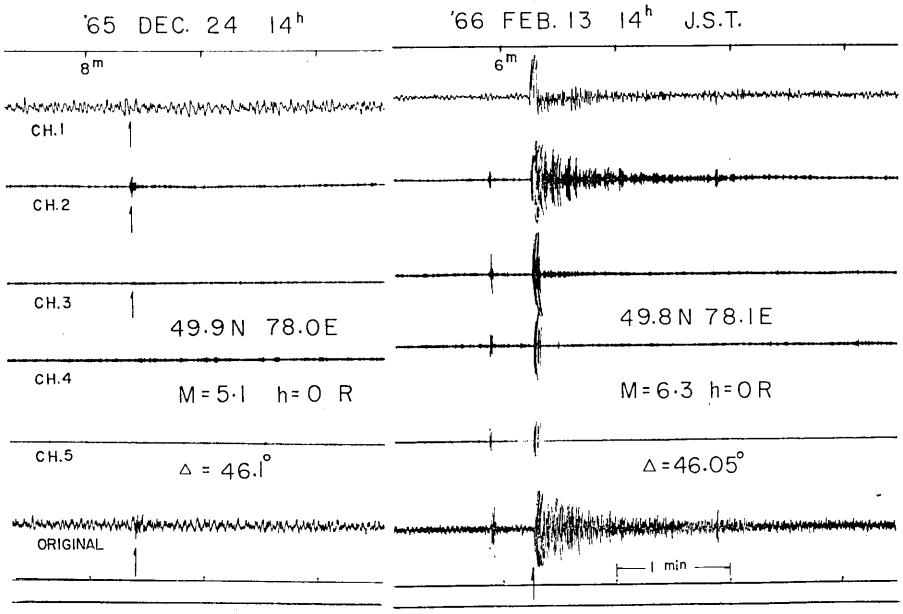

Fig. 12. Special example of the result of frequency analysis of the distant shocks. It is noticed that the amplitudes of the high frequency components are large in spite of the shallow focal depth.

Fig. 12 also shows an example of the result of analysis for some distant events. The first event in this figure is small and the background microseisms are large. On the other hand, the second event is too big, and during the few seconds after the initial motions, the pre-amplifier was saturated. Therefore, we could not obtain the spectrum of these wave portions. After the amplifier returned to normal operation, it is well recognized in this figure that the peak of the amplitude spectra appears in

11) J. Dorman, M. Ewing and J. Oliver, *Bull. Seism. Soc. Amer.*, **50** (1960), 87–115.

a high frequency channel where the center frequency is 2 cps in spite of the shallow focal depth (It is reported by U.S.C.G.S. as zero R).

We obtained the spectra for more than one hundred of the distant earthquakes. However, we could not find out the spectrum which contained the short period in channel 2 as much as indicated in this figure for the shallow earthquakes. We suppose, therefore, that these two exceptional events may be due to man-made explosions.

5. Summary

We found some interesting facts on the initial P waves of near and distant earthquakes through a frequency analysis method. They are summarized as follows:

1) The high frequency components of seismic waves suffered stronger attenuation than the lower frequency components in the propagation through the crust. Then, we obtained the attenuation curves of the amplitude ratio of different frequencies and calculated the value of the attenuation coefficient Q of the earth's crust. It is found that the lowest value of Q for P waves is about 500 in the crust and the upper-most mantle.

2) The ratio of the amplitude of seismic waves of 2 cps to that of frequencies lower than 1 cps generally becomes larger with the increase of focal depth. However, the amplitude ratio for the focal depth ranging from 100 and 200 km takes a very small value as compared with the values for the other focal depth ranges in the Fiji Islands region.

3) The suspected artificial teleseismic events show predominant amplitude in the 2 cps channel comparable with deep earthquakes and seem to differ significantly from the shallow natural earthquakes in spite of their shallow focal depths.

Acknowledgement

The writer wishes to express his thanks to Prof. Setumi Miyamura for his guidance and encouragement continuously given in the course of the present study. The writer also thanks Dr. Keiiti Aki for his valuable advice and Mr. Isao Nakamura for his kind help in the observation and data handling.

45. 地震波動の周波数分析 (1)

地震研究所 辻 浦 賢

近地地震ならびに遠震実体波についてのスペクトル構造をしらべるため，周波数分析装置を試作した．試作した装置はアナログ方式であり，0.5 サイクルから 40 サイクルの周波数範囲について，5組の濾波器により分類し，その出力はオリジナルの記録と共に6成分のインク書きオツシログラフによって連続記録をおこなっている．

1965年12月以後，筑波山に設置中の無線地震計をつかい，近地地震ならびに遠震実体波について観測し解析をおこなった．

主な結果は次の通りである．

1) 観測された近地地震の震源における平均的なスペクトルの比が一様であると仮定し，高周波成分と低周波成分の振巾比が，震源巨離の増加と共に減少することから地殻の Q を算出し，P 波についてその値 500 をえた．然し実際問題として，震源巨離の増加と共に大きな地震を対象としていることになり，その震源におけるスペクトルを考慮すると，上記の値は最低値であると考えられる．

2) 遠震実体波の初動に含まれる 2 サイクルを中心とした成分と，1 サイクル以下の周波数成分の振巾比は，一般に震源の深さの増加と共に増加する傾向にある．しかしその傾向は深さと共に一様ではなく，特にフイジー，トンガ島地域に発生する地震についてみると，ある深さ例えば，100 km ～200 km の範囲内では特に小さな値をもつ．

3) 遠震浅発地震であるにもかかわらず，特に 2 サイクルを中心とした周波数成分の卓越した地震を見出した．もちろん未だ地震波のスペクトル構造については多くの未知の問題が残されていると考えられるが，われわれの経験から，これらの地震は一般の自然地震とことなり人工的なものであると考えられる．